The Journal of the Astronautical Sciences, Vol. 58, No. 2, April–June 2011, pp. 221–240

Closed-Loop Control of Satellite Formations Using a Quasi-Rigid Body Formulation[1]

Christopher Blake[2] and Arun K. Misra[3]

Abstract

Satellites in formation work together to fulfill the role of a larger satellite. The purpose of this article is to develop a quasi-rigid body formulation for modeling and controlling such a formation as a single entity. In this article, a definition of a quasi-rigid body coordinate frame is presented, which, when attached to a formation, conveniently describes its orientation in space. Using this formulation, the equations of motion for a satellite formation are recast, and natural circular formations are expressed more succinctly. When the J_2 perturbation is considered, a correction factor on the formation's spin rate is introduced. The control of a satellite formation can effectively be separated into (1) a control torque to maintain the attitude and (2) control forces that maintain the rigidity of the formation. With this in mind, a nonlinear Lyapunov controller is derived using the formulation, which acts on the formation as a whole. Simulations validate this controller and illustrate its utility for maintaining circular formations, in particular, in the presence of gravitational perturbations.

Introduction

A satellite formation is a collection of smaller satellites working together to fulfill the role of a larger satellite. Such systems offer the possibility of cheaper, more versatile missions, but with a more complex system architecture. Many past, current, and future missions employ this concept. NASA's Earth-Observing-1 and Landsat-7 flew in formation to image the same ground track and demonstrated precision formation control. Cloudsat and CALIPSO are

[1]Initial version presented as Paper AAS 08-145 at the 18th AAS/AIAA Space Flight Mechanics Meeting, Galveston, Texas, January 2008.
[2]Master of Engineering, Department of Mechanical Engineering, McGill University, 817 Sherbrooke Street West, Montreal, Quebec H3A 2K6, Canada. Currently at MAYA Heat Transfer Technologies, 4999 St. Catherine Street West, Suite 400, Montreal, Quebec, H3Z 1T3, Canada.
[3]Thomas Workman Professor, Department of Mechanical Engineering, McGill University, 817 Sherbrooke Street West, Montreal, Quebec, H3A 2K6, Canada.

another pair of NASA satellites that take simultaneous measurements of the atmosphere to investigate the effects of clouds and aerosols on the Earth's climate. A formation flying strategy is used to keep a constant separation between the satellites. DLR placed the TanDEM-X satellite in formation with TerraSAR-X. The goal of the mission is to create a high accuracy global digital elevation model of the Earth. Can-X4 and Can-X5 designed by the Space Flight Laboratory of the University of Toronto will demonstrate new formation flying control algorithms for two elliptical formations. Finally, JC2Sat, a joint venture between the CSA and JAXA, will demonstrate the use of aerodynamic drag for formation control.

For a formation, the *relative* positions and velocities of the satellites are the primary concern. Much of the literature on formation flying has focused on the Hill-Clohessy-Wiltshire (HCW) equations [1, 2]. They approximately describe the relative motion of a satellite around a circular reference orbit in a two-body system. Sabol et al. [3] discussed four common formations that are analytical solutions to these dynamic equations. Yeh and Sparks [4] provided a geometric interpretation of these relative orbits and addressed certain control strategies. Schweighart and Sedwick [5] modified the HCW equations to obtain linear dynamics that also capture the J_2 perturbation. Vaddi and Vadali [6] compared three formation controllers based, in part, on the HCW equations.

Formation flying of satellites on more general elliptic orbits, where the eccentricity, e, is non-zero, was studied by Lawden [7] and Tschauner and Hempel [8]. Formations can also be described using differential mean orbital elements, around which different control strategies can be designed [9]. These approaches may be applied to formations of more than two satellites, but they describe the relative motion between only two satellites at a time, one the leader and the other the follower.

Because the purpose of formation flying is to emulate a larger satellite using smaller ones, it is natural to think of a formation as a single entity. Ren and Beard [10] described a formation as a virtual structure and developed a decentralized control architecture based on that idea. Tillerson et al. [11] defined a virtual center that captures the average motion of a formation, showing that controlling satellites around this point requires less effort. Clemente and Atkins [12] used the term "virtual rigid body" during the active control phases of the orbit of a three-dimensional formation. Rigid body formulations such as these often lead to non-Keplerian motion of the satellites, requiring non-zero feed-forward control effort.

The objective of this article is to mathematically describe a satellite formation to design controllers that treat the formation as a rigid body. A formation can be thought of as a rigid body when the relative positions of the satellites are perfectly maintained through some control effort. However, because these relative positions deviate, for example because of perturbation forces, the formation is only quasi-rigid. The idea of the quasi-rigid body was first proposed by Cochran et al. [13], and this article expands upon that idea.

The article begins by deriving the quasi-rigid body formulation for a satellite formation. Then, with reference to previous work [14], the equations of motion for a formation are derived. Natural circular formations are expressed more succinctly using the formulation. The analogy of the rigid body is used to develop a nonlinear closed-loop controller that acts on a formation as a whole. The controller is suitable

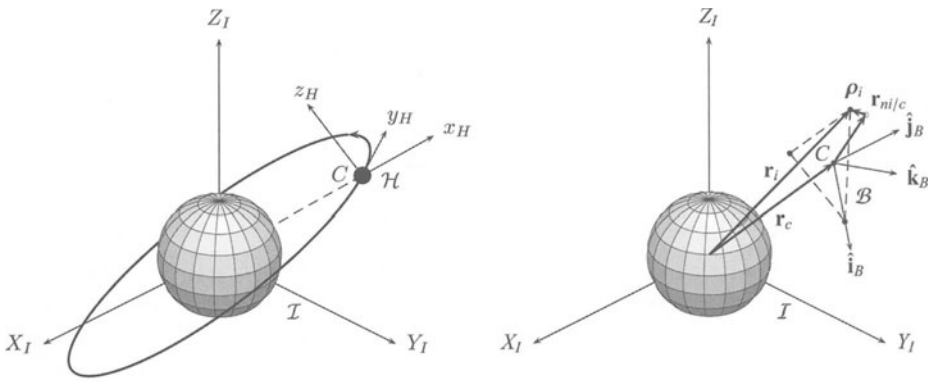

(a) Inertial and Local-Vertical-Local-Horizontal (b) Deputy Satellites within the QRB Frame

FIG. 1. Coordinate Frames

for large slewing maneuvers because it avoids introducing errors from linearizations or small-angle assumptions. Simulations illustrate the use of this controller for formation maintenance; formation reorientation is studied in a subsequent article. Overall, this article presents the viability of the quasi-rigid body formulation for controller design.

Quasi-Rigid Body Formulation

A satellite formation consists of N deputy satellites, numbered $i = 1, \ldots, N$, following a chief, denoted by C. It is assumed either that the trajectory of the chief is known analytically or that it can be propagated forward in time using a separate set of differential equations. Each deputy is modeled as a point mass, meaning that for the satellite formation, there are $3N$ degrees of freedom (DOF), three translational DOFs per deputy. The satellites travel with respect to an inertial coordinate frame, denoted by $\mathcal{I}$, located with its origin at the center of the Earth, the X_I-axis pointing towards the vernal equinox, and the Z_I-axis aligned with the North Pole. The motion of the chief around the Earth defines a second coordinate frame called the Local-Vertical-Local Horizontal (LVLH) Frame, denoted by $\mathcal{H}$, also known as the Hill frame. The origin of the LVLH frame is located at the center of mass of the chief satellite. The x_H-axis points in the radial direction along the line joining the center of the Earth with the chief, and the z_H-axis is parallel to the angular velocity vector of the chief's orbit. This is illustrated in Fig. 1(a). The basis vectors for this frame are $\{\hat{\mathbf{i}}_H, \hat{\mathbf{j}}_H, \hat{\mathbf{k}}_H\}$. For an unperturbed chief orbit, the LVLH frame rotates fully about its z_H-axis once per orbit.

The system is fully specified if the position vectors of the deputies relative to the origin of $\mathcal{I}$, $\mathbf{r}_i$ for all i, are known. Alternatively, the vector $\mathbf{r}_c$ along with $\mathbf{r}_{i/c}$ for all i also specifies the system, where the former is the position vector of the chief, and the latter is the position of the i^{th} deputy relative to the chief. This can be further decomposed

$$\mathbf{r}_i = \mathbf{r}_c + \mathbf{r}_{i/c} = \mathbf{r}_c + \mathbf{r}_{ni/c} + \boldsymbol{\rho}_i \tag{1}$$

where $\mathbf{r}_{ni/c}$ is some known desired or nominal location for the i^{th} deputy with respect to the chief and $\boldsymbol{\rho}_i$ is the deviation of the i^{th} deputy from that desired

position with respect to the chief. When $\boldsymbol{\rho}_i$ is known for each deputy, the system is fully specified.

The motivation behind the quasi-rigid body formulation is to characterize the orientation of the formation of satellites, and so three additional attitude coordinates are used to specify the system, completing the following set of generalized coordinates

$$\mathbf{X} = [\boldsymbol{\rho}_1^{\mathrm{T}} \quad \boldsymbol{\rho}_2^{\mathrm{T}} \quad \ldots \quad \boldsymbol{\rho}_N^{\mathrm{T}} \quad \theta_1 \quad \theta_2 \quad \theta_3]^{\mathrm{T}} \tag{2}$$

The three attitude coordinates $\{\theta_1, \theta_2, \theta_3\}$ specify the orientation of a coordinate frame associated with the formation, which will be called the quasi-rigid body (QRB) frame and is fully defined later. The frame is denoted by $\mathcal{B}$ and its origin is placed at the center of mass of the chief. The attitude coordinates, for example, can be a set of three independent Euler angles. Later, for the design of a nonlinear controller, quaternions will be used to define the attitude. Figure 1(b) illustrates the QRB frame attached to a planar formation of three deputies.

The QRB frame is reminiscent of the body frame, typically attached to a rigid body in order to describe its rotational dynamics. When modeling a flexible body, deflections with respect to that body frame are usually considered as independent from the rigid body motion. The same cannot be said here. The vector $\mathbf{X}$ is a set of constrained generalized coordinates because there are $3N + 3$ coordinates and only $3N$ DOFs. Hence, there must be a relationship between the attitude coordinates and the deviations of the deputies from their nominal positions. Determination of this relationship is an essential part of the QRB formulation. It specifies how the QRB frame is "attached" to the formation. The choice of how the frame is defined will consequently impose three constraints on the system.

The nominal relative position vectors and the deviation vectors are separated into components as

$$\mathbf{r}_{ni/c} = x_{ni}\hat{\mathbf{i}}_B + y_{ni}\hat{\mathbf{j}}_B + z_{ni}\hat{\mathbf{k}}_B \tag{3}$$

$$\boldsymbol{\rho}_i = u_i\hat{\mathbf{i}}_B + v_i\hat{\mathbf{j}}_B + w_i\hat{\mathbf{k}}_B \tag{4}$$

where $\{\hat{\mathbf{i}}_B, \hat{\mathbf{j}}_B, \hat{\mathbf{k}}_B\}$ are the basis vectors for the QRB frame, pointing along the x_B, y_B, and z_B-axes, respectively.

Blake [14] explores two general definitions for the basis vectors in terms of the deputy satellite positions: using principal axes, and using linear combinations of the relative position vectors. In this article, instead of using the relative positions of all N deputies in the definition, only two of the N deputies are used. The definition of the QRB frame is

$$\hat{\mathbf{i}}_B = \frac{\mathbf{r}_{1/c}}{\|\mathbf{r}_{1/c}\|} \qquad \hat{\mathbf{k}}_B = \frac{\mathbf{r}_{1/c} \times \mathbf{r}_{2/c}}{\|\mathbf{r}_{1/c} \times \mathbf{r}_{2/c}\|} \qquad \hat{\mathbf{j}}_B = \hat{\mathbf{k}}_B \times \hat{\mathbf{i}}_B \tag{5}$$

This leads to the following three constraints on the generalized coordinates

$$v_1 = 0 \qquad w_1 = 0 \qquad w_2 = 0 \tag{6}$$

where v_i and w_i are defined in equation (4). To be consistent, $y_{n1} = z_{n1} = z_{n2} = 0$. By attaching the frame to the formation this way, it means that the first deputy is confined to the x_B-axis and the second deputy is confined

to the XY-plane. The first two deputies are selected so that $\mathbf{r}_{1/c}$ and $\mathbf{r}_{2/c}$ are not parallel. The remaining deputies are not constrained. This is the definition of the QRB frame first introduced by Cochran et al. [13], though with a different labeling convention.

There is an important distinction between this work and the work of Cochran et al. [13]. In their work, the origin of the QRB frame is aligned with the center of mass of the formation, imposing additional constraints on the generalized coordinates. This means that in the local QRB frame, it is possible for $N - 1$ deputies to change position independently, but the N^{th} deputy must change position to keep the center of mass at the origin. Cochran et al. [13] go one step further and confine the motion of the center of mass to a circular orbit, which simplifies the dynamics, but ultimately just prescribes the motion of the N^{th} deputy. In reality, the center of mass of the system will follow a more complex trajectory about the Earth because of the perturbations experienced by the individual deputies. In this study, the origin of the QRB frame is aligned with a chief satellite, which can follow any path, allowing all the deputies to move freely. The chief could be the combiner spacecraft in a separated spacecraft interferometer. Or, the chief may simply be an imaginary point relative to which the deputies move.

Equations of Motion

For the QRB formulation to be useful in terms of system modeling or controller synthesis, the QRB frame must be incorporated into the system dynamics. Cochran et al. [13] derived the equations of motion for a distributed satellite system using Newton's Second Law. Here, they are derived using a Lagrangian approach and it is shown that an angular momentum equation for the system falls out naturally.

The generalized coordinates and generalized speeds that specify the system are, respectively,

$$\mathbf{q} = [\boldsymbol{\rho}_1^{\mathrm{T}} \quad \boldsymbol{\rho}_2^{\mathrm{T}} \quad \cdots \quad \boldsymbol{\rho}_N^{\mathrm{T}} \quad \theta_1 \quad \theta_2 \quad \theta_3]^{\mathrm{T}} \tag{7}$$

$$\mathbf{p} = [\mathring{\boldsymbol{\rho}}_1^{\mathrm{T}} \quad \mathring{\boldsymbol{\rho}}_2^{\mathrm{T}} \quad \cdots \quad \mathring{\boldsymbol{\rho}}_N^{\mathrm{T}} \quad \boldsymbol{\omega}_B^{\mathrm{T}}]^{\mathrm{T}} \tag{8}$$

where ω_B is the angular velocity of the QRB frame. Together, these are the *QRB states*, $\mathbf{x}$. All the vectors are expressed in the QRB frame, but it is realized that by enforcing the constraints in equation (6), $\boldsymbol{\rho}_1$ contains only one non-zero component and $\boldsymbol{\rho}_2$ only two non-zero components. Hence, together they only contribute three generalized coordinates, and $\mathbf{q}$ is an independent set of $3N$ generalized coordinates. The vector notation for deputies 1 and 2 is retained only for the sake of uniformity.

The time derivatives of the generalized coordinates are related to the generalized speeds by

$$\frac{\mathrm{d}}{\mathrm{d}t}\mathbf{q} = [D(\mathbf{q})]\mathbf{p} = \begin{bmatrix} [E]_{(3N-3)\times(3N-3)} & [0]_{(3N-3)\times 3} \\ [0]_{3\times(3N-3)} & [B(\boldsymbol{\theta}_B)] \end{bmatrix} \mathbf{p} \tag{9}$$

where matrix $[E]$ is the identity matrix, and matrix $[B(\boldsymbol{\theta}_B)]$ is obtained from $(\mathrm{d}/\mathrm{d}t)\boldsymbol{\theta}_B = [B(\boldsymbol{\theta})]\boldsymbol{\omega}_B$, and depends on the choice of Euler angles (see [15]).

The inertial position of the i^{th} deputy satellite is given in equation (1); the velocity of the i^{th} deputy satellite, expressed in the QRB frame, is given by

$$\dot{\mathbf{r}}_i = \frac{\mathrm{d}}{\mathrm{d}t}\mathbf{r}_i = \dot{\mathbf{r}}_c + \mathring{\mathbf{r}}_{i/c} + [\boldsymbol{\omega}_B^{\times}]\mathbf{r}_{i/c} \tag{10}$$

The superscript $\times$ indicates a skew-symmetric cross-product matrix formed by the components of the vector the symbol modifies. An over-dot signifies a time derivative in the inertial frame, whereas an over-circle signifies a time derivative in the QRB frame, i.e., a local derivative.

The kinetic energy of the system can be expressed as a function of the generalized coordinates and their derivatives, $T(\mathbf{q}, (\mathrm{d}/\mathrm{d}t)\mathbf{q}, t)$, or as a function of the generalized coordinates and the generalized speeds, $\bar{T}(\mathbf{q}, \mathbf{p}, t)$. In the latter case, the dependency of the generalized speeds on the generalized coordinates must be accounted for in Lagrange's equation. Letting $[C]^{\mathrm{T}} = [D]^{-1}$, the modified version of Lagrange's equations of motion is [15]

$$\frac{\mathrm{d}}{\mathrm{d}t}\left(\frac{\partial \bar{T}}{\partial \mathbf{p}}\right) + [D]^{\mathrm{T}}([\dot{C}] - [G])\frac{\partial \bar{T}}{\partial \mathbf{p}} - [D]^{\mathrm{T}}\frac{\partial \bar{T}}{\partial \mathbf{q}} = [D]^{\mathrm{T}}\mathbf{Q} \tag{11}$$

where

$$[G] = \begin{bmatrix} \mathbf{p}^{\mathrm{T}}[D]^{\mathrm{T}}\left[\dfrac{\partial [C]}{\partial \mathbf{q}_1}\right] \\ \vdots \\ \mathbf{p}^{\mathrm{T}}[D]^{\mathrm{T}}\left[\dfrac{\partial [C]}{\partial \mathbf{q}_n}\right] \end{bmatrix} \tag{12}$$

and $\mathbf{Q}$ is the column vector of generalized forces. The kinetic energy of the system is then

$$\bar{T} = \sum_{i=1}^{N} \frac{1}{2} m_i \dot{\mathbf{r}}_i^{\mathrm{T}} \dot{\mathbf{r}}_i = \frac{1}{2}\mathbf{p}^{\mathrm{T}}[M(\mathbf{q})]\mathbf{p} + \beta(\mathbf{q})^{\mathrm{T}}\mathbf{p} + \bar{T}_0 \tag{13}$$

with

$$[M(\mathbf{q})] = \begin{bmatrix} m_1[E] & [0] & \cdots & [0] & m_1[\mathbf{r}_{1/c}^{\times}]^{\mathrm{T}} \\ [0] & m_2[E] & \cdots & [0] & m_2[\mathbf{r}_{2/c}^{\times}]^{\mathrm{T}} \\ \vdots & \vdots & \ddots & \vdots & \vdots \\ [0] & [0] & \cdots & m_N[E] & m_N[\mathbf{r}_{N/c}^{\times}] \\ m_1[\mathbf{r}_{1/c}^{\times}] & m_2[\mathbf{r}_{2/c}^{\times}] & \cdots & m_N[\mathbf{r}_{N/c}^{\times}] & [I] \end{bmatrix} \tag{14}$$

$$\beta(\mathbf{q}) = \begin{bmatrix} m_1(\dot{\mathbf{r}}_c + \mathring{\mathbf{r}}_{n1/c}) \\ \vdots \\ m_N(\dot{\mathbf{r}}_c + \mathring{\mathbf{r}}_{nN/c}) \\ \sum_{i=1}^{N} m_i[\mathbf{r}_{i/c}^{\times}](\dot{\mathbf{r}}_c + \mathring{\mathbf{r}}_{ni/c}) \end{bmatrix} \tag{15}$$

$$\bar{T}_0 = \sum_{i=1}^{N} \left\{ \frac{1}{2} m_i \dot{\mathbf{r}}_c^{\mathrm{T}} \dot{\mathbf{r}}_c + m_i \dot{\mathbf{r}}_c^{\mathrm{T}} \mathring{\mathbf{r}}_{ni/c} + \frac{1}{2} m_i \mathring{\mathbf{r}}_{ni/c}^{\mathrm{T}} \mathring{\mathbf{r}}_{ni/c} \right\} \tag{16}$$

and where m_i is the mass of the i^{th} deputy and $[I]$ is the "moment of inertia" of the formation about the chief, given by

$$[I] = \sum_{i=1}^{N} m_i (\mathbf{r}_{i/c}^{\mathrm{T}} \mathbf{r}_{i/c} [E] - \mathbf{r}_{i/c} \mathbf{r}_{i/c}^{\mathrm{T}}) \tag{17}$$

A detailed derivation of each term in the modified Lagrange equations (11) can be found in [14]. Using the Jacobi Identity to combine the terms, the EOMs for a satellite formation using the QRB formulation are

$$\mathring{\boldsymbol{\rho}}_i - [\dot{\boldsymbol{\omega}}_B^{\times}] \mathbf{r}_{i/c} = -2[\boldsymbol{\omega}_B^{\times}] \mathring{\mathbf{r}}_{i/c} - [\boldsymbol{\omega}_B^{\times}][\boldsymbol{\omega}_B^{\times}] \mathbf{r}_{i/c} - \mathring{\mathbf{r}}_{ni/c} + \frac{1}{m_i} \mathbf{F}_i - \ddot{\mathbf{r}}_c \quad i = 1, \ldots, N \tag{18a}$$

$$[I]\dot{\boldsymbol{\omega}}_B + \sum_{i=1}^{N} m_i [\mathbf{r}_{i/c}^{\times}] \mathring{\boldsymbol{\rho}}_i = -2 \sum_{i=1}^{N} m_i [\mathbf{r}_{i/c}^{\times}][\boldsymbol{\omega}_B^{\times}] \mathring{\mathbf{r}}_{i/c} - [\boldsymbol{\omega}_B^{\times}][I]\boldsymbol{\omega}_B - \sum_{i=1}^{N} m_i [\mathbf{r}_{i/c}^{\times}] \mathring{\mathring{\mathbf{r}}}_{ni/c} - \sum_{i=1}^{N} m_i [\mathbf{r}_{i/c}^{\times}] \ddot{\mathbf{r}}_c + \boldsymbol{\Gamma} \tag{18b}$$

$$\dot{\boldsymbol{\theta}}_B = [B(\boldsymbol{\theta}_B)] \boldsymbol{\omega}_B \tag{18c}$$

where $\mathbf{F}_i = \mathbf{F}_{gi} + \mathbf{F}_{pi} + \mathbf{F}_{ci}$ is the sum of the forces acting on the i^{th} deputy, $\mathbf{F}_{gi} = -(m_i \mu / r_i^3) \mathbf{r}_i$ is the gravitational force, $\mathbf{F}_{pi}$ accounts for any perturbation forces such as those caused by J_2 or atmospheric drag, and $\mathbf{F}_{ci}$ is the control effort. The torque $\boldsymbol{\Gamma}$ is the sum of the moments of all these forces about the origin of the QRB frame. Equation (18c) is included with the equations of motion to relate the rotational generalized coordinates and speeds. Nothing in equation (18) dictates that Euler angles must parameterize the orientation, so equation (18c) can be replaced by the kinematic relationship for any set of attitude coordinates, for example, quaternion components.

In equation (18a), three of the scalar differential equations are dropped because v_1, w_1, and w_2 are identically zero. Notice that if all the deviations are held to zero, the nominal relative position vectors are constant in the QRB frame, and the chief is located at the center of mass of the formation, equation (18b) collapses to Euler's rotational equation for a rigid body:

$$[I_c]\, \dot{\omega}_B = -[\omega_B^{\times}]\, [I_c]\, \omega_B + \boldsymbol{\Gamma} \tag{19}$$

The goal of a control scheme designed using the QRB formulation is to achieve this formation "rigidity" and to orient the formation as if it was a rigid body. Rigidity is important when scientific data collection is to occur during formation reorientation, when collision avoidance is a prime concern, or when sensor lock between satellites needs to be maintained.

Natural Solutions Using the Formulation

The Hill-Clohessy-Wiltshire (HCW) equations [1, 2] describe the relative motion between a single deputy and chief satellite under the assumptions that (1) intersatellite distances are small compared to the semimajor axis of the chief orbit and (2) the chief is on an unperturbed circular orbit.

When the deputies in a satellite formation all lie on the same relative orbit, the QRB formulation becomes a powerful way of describing the formation. This is particularly true when all the deputies remain equidistant from the chief in a circular relative orbit. Using QRB states, this formation is given by

$$[R_{\mathfrak{B}/\mathfrak{H}}] = [R_z(nt + \phi_0)][R_y(\pm 2\pi/3)] \tag{20}$$

$$\boldsymbol{\omega}_B = n\hat{\mathbf{k}}_H + n\hat{\mathbf{k}}_B = -\frac{\sqrt{3}}{2} n \cos(nt + \phi_0)\hat{\mathbf{i}}_B + \frac{\sqrt{3}}{2} n \sin(nt + \phi_0)\hat{\mathbf{j}}_B + \frac{1}{2} n\hat{\mathbf{k}}_B \tag{21}$$

$$\mathbf{r}_{ni/c} = R_o \cos \psi_i \hat{\mathbf{i}}_B + R_o \sin \psi_i \hat{\mathbf{j}}_B \quad i = 1, \ldots, N \tag{22}$$

$$\mathring{\mathbf{r}}_{ni/c} = \mathring{\mathring{\mathbf{r}}}_{ni/c} = 0 \quad i = 1, \ldots, N \tag{23}$$

The term $[R_{\mathfrak{B}/\mathfrak{H}}]$ is the direction cosine matrix (DCM) relating the basis vectors of the LVLH frame to the basis vectors of the QRB frame. The matrices $[R_y]$ and $[R_z]$ are fundamental rotation matrices about body-fixed y- and z-axes, respectively. The nominal vectors, $\mathbf{r}_{ni/c}$, are used to describe the natural relative positions within the QRB frame so that the vectors, $\boldsymbol{\rho}_i$, represent deviations from this natural relative orbit. The distribution of the deputies within the QRB frame is determined by the choice of offset angles ψ_i, and an additional offset ϕ_0 can be used to set the initial spin angle of the circular formation about the z_B-axis.

The advantage of describing a formation this way is that instead of having separate trajectories for each deputy, the deputies are fixed within the QRB frame and it is the QRB frame that moves and rotates. Furthermore, the frame by itself characterizes the pointing direction of the entire formation.

The natural circular formation assumes zero perturbation forces, however in reality, this is not the case. For example, the J_2 perturbation can cause deputy satellites to drift away from the chief in the along-track or y_H-direction. In the presence of J_2, bounded relative motion solutions do exist in terms of differential mean orbital elements [16], but an expression of these in terms of QRB states would be overly complicated.

However, Vadali et al. [17] proposed a modification to the HCW equations to account for J_2. They replaced the mean orbital rate of the chief, n, with a perturbed mean orbital rate, $\bar{n}_c$, as

$$\bar{n}_c = \frac{\mathrm{d}}{\mathrm{d}t}\bar{\omega}_c + \frac{\mathrm{d}}{\mathrm{d}t}\bar{M}_c \tag{24}$$

which is the sum of the rates of change of the mean orbital elements of the chief argument of perigee, $\bar{\omega}_c$, and mean anomaly, $\bar{M}_c$. They are both functions of J_2. The derivation of Vadali et al. [17] also produces a disturbance function in the z_H-direction. Because of the similarity with the HCW equations, they proposed a

reference trajectory similar to the closed-form periodic solutions in [4], though with an angular rate that also contains a correction factor

$$n^* = \bar{n}_c + \dot{\alpha} \tag{25}$$

where $\dot{\alpha}$ is meant to detune the natural frequency of the z_H-motion from the frequency of the disturbance function. They went on to develop a linear controller using these equations of motion and showed the fuel savings it provides.

This work suggests that there is a "near-natural" circular formation in the presence of the J_2 perturbation, in which the angular velocity of the QRB is corrected by an amount of the order of J_2. Again, this correction to the formation trajectory is easily expressed using the QRB formulation: the angular velocity of the QRB frame becomes

$$\boldsymbol{\omega}_{B/H} = n^* \hat{\mathbf{k}}_H + n^* \hat{\mathbf{k}}_B \tag{26}$$

Open-Loop Control of Circular Formations

Deputy satellites distributed symmetrically about the same relative circular orbit form a quasi-rigid formation that essentially mimics the motion of an axisymmetric rigid body. Under the simplifying assumptions of a circular chief orbit and small intersatellite distances, the deputies require no control forces to maintain their natural relative orbit trajectories. However, Blake [14] shows that even if the deputies are placed on unnatural or forced trajectories, continuing to view the formation as quasi-rigid leads to an open-loop control scheme. What follows is a brief summary of the findings and more details can be found in [14].

Blake [14] shows how the motion of the QRB frame in a natural circular formation is a combination of precession, nutation, and spin. The QRB precesses about the LVLH frame z_H-axis and spins about the QRB z_B-axis, while maintaining a constant nutation angle about the LVLH y_H-axis. When the spin rate is equal to the orbital rate of the chief, $n = \sqrt{\mu/r_c^3}$, the gravity gradient torque experienced by the formation is sufficient to maintain the constant nutation angle. When the spin rate is not n or the nutation angle changes, additional control effort is required.

To maintain such a forced QRB formation trajectory, the open-loop control effort can effectively be separated into a control torque that maintains the orientation of the formation as a whole, and a set of control forces applied to the deputies that maintain the rigidity of the QRB, but that apply no net moment. However, without any state feedback, the open-loop scheme is unable to regulate any state errors, as shown through simulations in [14]. This motivates the development of the closed-loop controller in the next section.

Nonlinear Closed-Loop Control

This section shows how the QRB formulation can be used to design a *closed-loop* nonlinear control scheme that acts on a formation as a single entity. The technique of feedback linearization is used to cancel out nonlinear terms and obtain linear dynamic equations for the state error. This article does not consider a specific mission for the controller design. As such, several simplifying assumptions are made:

1. The mass of each satellite is much larger than the mass of on-board fuel. Therefore, the change in the system mass when fuel is expended can be neglected.
2. On-board thrusters can produce continuous thrust in all three coordinate directions of the QRB frame.
3. The satellites can be treated as point masses.
4. The location of the chief satellite or reference point is known.
5. State measurements are perfect, i.e., there are no navigation errors.

For real-world missions, limited thrust capabilities and navigational errors are important drivers of controller performance. Future studies of QRB controllers would need to take these into account.

Letting the subscript D stand for "desired," the desired orientation for the QRB frame is given by the quaternion, $\bar{q}_D$, whereas the desired angular velocity is $\boldsymbol{\omega}_D$. The desired position vector of the i^{th} deputy in the QRB frame is the nominal position vector, $\mathbf{r}_{ni/c}$. The errors in position and speed used for the controller are then

$$\Delta\mathbf{q} = \mathbf{q} - \mathbf{q}_D = [\boldsymbol{\rho}_1^{\mathrm{T}} \quad \cdots \quad \boldsymbol{\rho}_N^{\mathrm{T}} \quad \varepsilon^{\mathrm{T}}]^{\mathrm{T}} \tag{27}$$

$$\Delta\mathbf{p} = \mathbf{p} - \mathbf{p}_D = [\mathring{\boldsymbol{\rho}}_1^{\mathrm{T}} \quad \cdots \quad \mathring{\boldsymbol{\rho}}_N^{\mathrm{T}} \quad \boldsymbol{\omega}_{B/D}^{\mathrm{T}}]^{\mathrm{T}} \tag{28}$$

where $\boldsymbol{\omega}_{B/D}$ is the angular velocity of the QRB with respect to the desired frame, while $\boldsymbol{\varepsilon}$ is the vector component of the quaternion, $\bar{q}_{B/D} = [q_0 \quad \boldsymbol{\varepsilon}^{\mathrm{T}}]^{\mathrm{T}}$, representing the error in orientation. When the components of this vector are all zero, the orientation error disappears. Thus, the goal of the controller is to drive the state error $\Delta\mathbf{x} = [\Delta\mathbf{q}^{\mathrm{T}} \quad \Delta\mathbf{p}^{\mathrm{T}}]^{\mathrm{T}}$ to zero making all the deviations, along with the orientation and angular velocity error, equal to zero. The speed error and the rate of change of the position error are related by

$$\Delta\dot{\mathbf{q}} = [H]\Delta\mathbf{p} = \begin{bmatrix} [E_{(3N-3)\times(3N-3)}] & [0_{(3N-3)\times 1}] \\ [0_{1\times(3N-3)}] & \tfrac{1}{2}\,[B(\bar{q}_{B/D})] \end{bmatrix} \Delta\mathbf{p} \tag{29}$$

where $[B] = q_0[E] + [\boldsymbol{\varepsilon}^{\times}]$ relates the angular velocity error to the quaternion error rate.

A candidate Lyapunov function for the system is selected as

$$L = \tfrac{1}{2}\,\Delta\mathbf{p}^{\mathrm{T}}\Delta\mathbf{p} + \tfrac{1}{2}\,\Delta\mathbf{q}^{\mathrm{T}}[K]\Delta\mathbf{q} \tag{30}$$

where $[K]$ is a symmetric positive definite matrix. The function L is then a positive definite function of the system state, $\mathbf{x}$, about the desired state, $\mathbf{x}_D$. Setting the rate of change of this function equal to $-\Delta\mathbf{p}^{\mathrm{T}}[P]\Delta\mathbf{p}$, where $[P]$ is also symmetric positive definite, makes $\dot{L}$ negative semi-definite so that L satisfies the criteria for a Lyapunov function. Then, by Lyapunov's Direct Method, the QRB system is stable about the desired state trajectory.

The dynamic equation for the state error then becomes

$$\Delta\dot{\mathbf{p}} + [P]\Delta\mathbf{p} + [H]^{\mathrm{T}}[K]\Delta\mathbf{q} = \mathbf{0} \tag{31}$$

The EOMs in equation (18) can be written compactly as

$$[M(\mathbf{q})]\dot{\mathbf{p}} = \boldsymbol{\Upsilon}(\mathbf{q}, \mathbf{p}, t) + \mathbf{Q}_c \tag{32}$$

where $[M(\mathbf{q})]$ is the symmetric mass matrix from equation (14), $\mathbf{Q}_c$ is the vector of generalized control forces, and Υ simply represents all remaining terms. Substituting equations (28) and (32) into equation (31), and solving for the control forces gives

$$\mathbf{Q}_c = \begin{bmatrix} \mathbf{F}_c \\ \mathbf{\Gamma}_c \end{bmatrix} = -[M(\mathbf{q})][H]^{\mathrm{T}}[K]\Delta\mathbf{q} - [M(\mathbf{q})][P]\Delta\mathbf{p} - \Upsilon + [M(\mathbf{q})]\dot{\mathbf{p}}_D \tag{33}$$

where

$$\dot{\mathbf{p}}_D = [\mathbf{0}^{\mathrm{T}} \quad (\dot{\boldsymbol{\omega}}_D - [\boldsymbol{\omega}_B^{\times}]\boldsymbol{\omega}_D)^{\mathrm{T}}]^{\mathrm{T}} \tag{34}$$

Equation (33) is the *nonlinear Lyapunov controller*. The role of each term in this control expression is apparent. The first term is the position error feedback whereas the second term is the velocity error feedback. The selection of matrices $[K]$ and $[P]$ determines the dynamics of the state error. Subtracting Υ cancels out the nonlinear terms of the dynamic equation, and so it provides feedback linearization. The last term is the control effort needed to maintain the desired state trajectory. Using the Theorem on Asymptotic Stability [18], it can be shown that this controller is asymptotically stable. Thus, provided Υ accurately models the nonlinear dynamics (gravity, perturbations), any deviations or orientation errors will be driven to zero by the controller. In practice, of course, a perfect model is not typically available.

Assuming $[K]$ and $[P]$ are block diagonal, the control law can be rewritten fully as

$$\begin{aligned} \mathbf{F}_{ci} = {} & -m_i[K_i]\boldsymbol{\rho}_i - m_i[P_i]\mathring{\boldsymbol{\rho}}_i + 2m_i[\boldsymbol{\omega}_B^{\times}]\mathring{\mathbf{r}}_{i/c} + m_i[\boldsymbol{\omega}_B^{\times}][\boldsymbol{\omega}_B^{\times}]\mathbf{r}_{i/c} + m_i\mathring{\mathring{\mathbf{r}}}_{ni/c} \\ & + m_i\ddot{\mathbf{r}}_c - \mathbf{F}_{gi} - m_i[\mathbf{r}_{i/c}^{\times}](\boldsymbol{\omega}_D - [\boldsymbol{\omega}_B^{\times}]\boldsymbol{\omega}_D) \\ & + \frac{1}{2}m_i[\mathbf{r}_{i/c}^{\times}][B]^{\mathrm{T}}[K_{\omega}]\boldsymbol{\epsilon} + m_i[\mathbf{r}_{i/c}^{\times}][P_{\omega}]\boldsymbol{\omega}_{B/D} \quad i = 1, \ldots, N \end{aligned} \tag{35a}$$

$$\begin{aligned} \mathbf{\Gamma}_c = {} & -\frac{1}{2}[I][B]^{\mathrm{T}}[K_{\omega}]\boldsymbol{\epsilon} - [I][P_{\omega}]\boldsymbol{\omega}_{B/D} + 2\sum_{i=1}^{N} m_i[\mathbf{r}_{i/c}^{\times}][\boldsymbol{\omega}_B^{\times}]\mathring{\mathbf{r}}_{i/c} + [\boldsymbol{\omega}_B^{\times}][I]\boldsymbol{\omega}_B \\ & + \sum_{i=1}^{N} m_i[\mathbf{r}_{i/c}^{\times}]\mathring{\mathring{\mathbf{r}}}_{ni/c} + \sum_{i=1}^{N} m_i[\mathbf{r}_{i/c}^{\times}]\ddot{\mathbf{r}}_c - \mathbf{\Gamma}_g + [I]\dot{\boldsymbol{\omega}}_D - [I][\boldsymbol{\omega}_B^{\times}]\boldsymbol{\omega}_B \\ & - \sum_{i=1}^{N} m_i[\mathbf{r}_{i/c}^{\times}][K_i]\boldsymbol{\rho}_i - \sum_{i=1}^{N} m_i[\mathbf{r}_{i/c}^{\times}][P_i]\mathring{\boldsymbol{\rho}}_i \end{aligned} \tag{35b}$$

Studying this control law, it would appear that the control torque applied to the QRB is obtained by summing the moments of the control forces about the chief, i.e.

$$\mathbf{\Gamma}_c = \sum_{i=1}^{N}[\mathbf{r}_{i/c}^{\times}]\mathbf{F}_{ci} \tag{36}$$

However, there is a subtlety. Recall that v_1, w_1, and w_2 are identically zero from the constraints in equation (6), and so they are not generalized coordinates. As a consequence, there are three force components left unspecified in equation (35a). After subtracting the moments contributed by all the known force components

from the control torque, $\mathbf{\Gamma}_c$, any remaining torque must be supplied by the yet unspecified force components. Symbolically,

$$\mathbf{\Gamma}_{c,\text{rem}} = \mathbf{\Gamma}_c - \sum_{i=1}^{N} [\mathbf{r}_{i/c}^{\times}]\mathbf{F}_{ci,\text{known}} = [\mathbf{r}_{1/c}^{\times}]\mathbf{F}_{c1,\text{free}} + [\mathbf{r}_{2/c}^{\times}]\mathbf{F}_{c2,\text{free}} \tag{37}$$

$$= \begin{bmatrix} -z_{n1} - w_1 & y_{n1} + v_1 & y_{n2} + v_2 \\ 0 & -x_{n1} - u_1 & -x_{n2} - u_2 \\ x_{n1} + u_1 & 0 & 0 \end{bmatrix} \begin{bmatrix} F_{c1,y} \\ F_{c1,z} \\ F_{c2,z} \end{bmatrix}$$

which can be solved. Hence, the Lyapunov controller does specify all the control forces needed to drive the deviations and orientation error to zero. Like with the open-loop scheme in [14], the control torque, $\mathbf{\Gamma}_c$, applied to the formation is generated by the moments of the individual control forces.

Gain Selection

If the feedback gain matrices, $[K]$ and $[P]$, are diagonal, and if one takes $[B]^{\mathrm{T}} \approx [E]$ for small orientation error, the dynamic equation for the error, equation (31), can be decoupled into second-order linear constant-coefficient differential equations. For the deviation errors, $\boldsymbol{\rho}_i$, the natural frequency and damping ratio are $\varpi_n = \sqrt{K_i}$ and $\zeta = P_i/(2\sqrt{K_i})$ whereas for the orientation error, ε, they are $\varpi_n = \sqrt{K_\omega}/2$ and $\zeta = P_\omega/\sqrt{K_\omega}$. Provided the damping ratio, ζ, is less than 1, the settling time for the error is $T_s \approx 4/(\varpi_n \zeta) = 8/P$. Hence, the values along the diagonal for matrices $[K]$ and $[P]$ can be chosen so that the system meets imposed performance specifications.

Simulations

The dynamic model of a satellite formation using the QRB formulation was validated through simulation in [14]. Thus, in this section, maintenance fuel trends for the nonlinear Lyapunov controller are examined, its performance is compared with an example from the literature, and it is tested in the presence of gravitational perturbations.

Implementation

For these simulations, the dynamic equations of motion were first non-dimensionalized so that changing absolute system parameters did not affect the relative magnitudes of the system state variables, and simulation tolerances could be set in a consistent manner. Whereas the controller was derived from the QRB dynamic model, the motion of each satellite was propagated forward using Newton's Law of Gravitation, with control forces and, where noted, gravitational perturbations (J_2 through J_4) applied. Matlab's differential equation solver, ode113, was used to simulate the system. This solver provides a good compromise between speed and accuracy. It is an Adams-Bashforth-Moulton multi-step solver that proves to be more efficient than ode45 for this system. A relative tolerance of 1×10^{-9} was used, with an absolute tolerance of 1×10^{-12}

Simulations involving the Lyapunov controller assumed that the system states could be measured perfectly, that is, navigation errors were not considered. As designed, the Lyapunov controller expects feedback of QRB states, $\mathbf{x}$, but the range

and rate measurements from on-board sensors typically yield inertial states for the chief and the deputies. However, these can be transformed into QRB states; see [14] for details.

The nominal formation was the natural circular formation with radius $R_o = 1$ km and orientation $[R_{\mathcal{D}/\mathcal{H}}] = [R_y(2\pi/3)]$. The deputies in the formation each had a mass of 100 kg, which is a reasonable size for a microsatellite, and they were symmetrically arranged around the circle

$$\mathbf{r}_{ni/c} = R_o \cos \psi_i \hat{\mathbf{i}}_B + R_o \sin \psi_i \hat{\mathbf{j}}_B \qquad \psi_i = \frac{2\pi}{N}(i-1), \quad i = 1, \ldots, N \tag{38}$$

Controller gain matrices were selected so that the same value was along the diagonal

$$[K] = Kn^2\,[E] \qquad [P] = Pn\,[E] \tag{39}$$

The gain values, K and P, are non-dimensional, hence the factors of n^2 and n in equation (39).

Maintenance Δv Trends

Several simulations were run to examine the effectiveness of the Lyapunov controller. The average Δv per orbit required to maintain a formation of three deputies was obtained for ranges of the simulation parameters. The trend plots are presented in Fig. 2.

As the size of the chief orbit increased, the assumption $\|\mathbf{r}_{i/c}\| \ll \|\mathbf{r}_c\|$ for a natural circular formation became more valid. The circular formation became easier to maintain, and the Δv per satellite decreased. As the formation size increased, the assumption became less valid, and more Δv was required for formation-keeping. More Δv was required as the eccentricity of the chief orbit increased because the natural circular formation also assumes a circular chief orbit. As seen in Fig. 2(b), the Δv consumption differed for each deputy. The distribution of the deputies within the QRB frame along with the initial spin angle of the frame determines their initial conditions within the inertial frame, and for an eccentric chief orbit, this impacts the Δv consumption.

Validation with Example from Literature

Vaddi and Vadali [6] studied three types of controllers for formation flying: a Lyapunov controller, an LQR controller, and a period-matching controller. The first two were derived based on the relative motion dynamics between a single deputy and a chief on a circular orbit. Their work provides a good comparison baseline for the Lyapunov controller in this article.

Vaddi and Vadali [6] measured the fuel consumed by their controllers to maintain the deputy on a projected-circular relative orbit about the chief. Though this is actually an elliptical relative orbit, the QRB formulation can still be used to describe the motion of the deputy. They started the deputy with two sets of initial conditions. The characteristic size of their formation was 10 km, and the chief was placed on a circular orbit ($e = 0$) of semimajor axis 7100 km, which is a low-Earth orbit. The measure of the fuel consumption for the deputy was

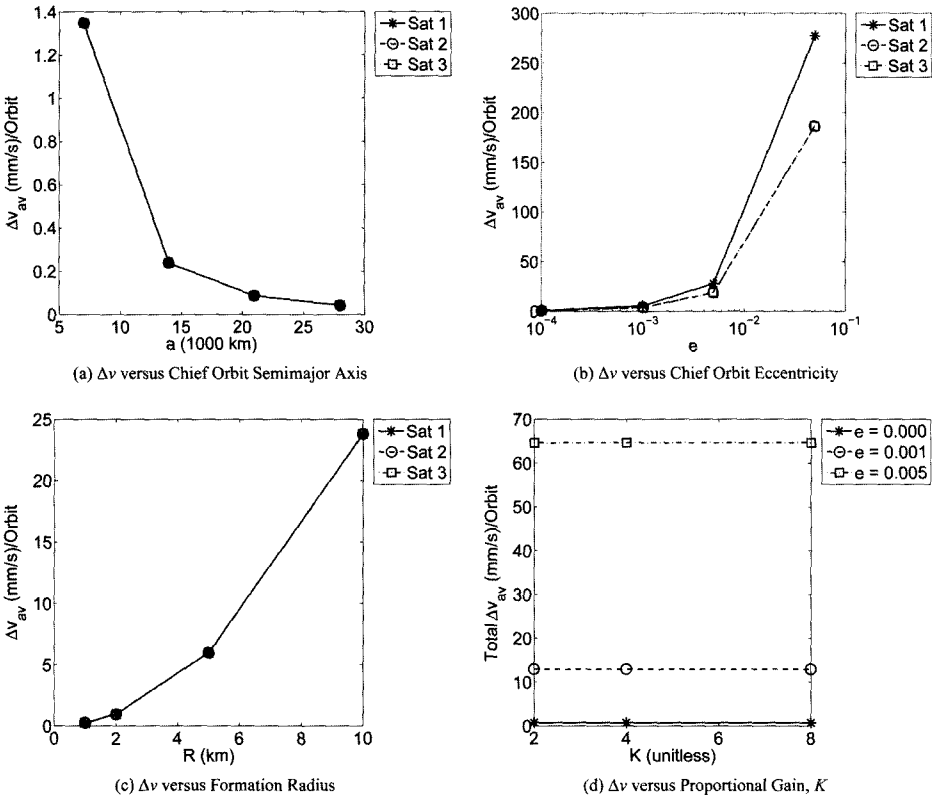

(a) Δv versus Chief Orbit Semimajor Axis

(b) Δv versus Chief Orbit Eccentricity

(c) Δv versus Formation Radius

(d) Δv versus Proportional Gain, K

FIG. 2. Average Maintenance Δv Trends for Lyapunov Controller with Perfect Internal Model

$$\int_0^{T_f} \left\| \frac{F_{ci}}{m_i} \right\|^2 \mathrm{d}t \tag{40}$$

and was reported in units of m^2/s^3/year.

Using the same simulation parameters, the projected-circular relative orbit was simulated using the QRB Lyapunov controller. Because this controller employs the QRB formulation, it acts on an entire formation containing two or more deputies, whereas the controllers developed by Vaddi and Vadali [6] act on a single deputy at a time. To compare fuel consumption for individual deputies, four deputies were distributed symmetrically within the QRB frame such that two of them began with the same initial conditions used by Vaddi and Vadali [6] in their study. The non-dimensional Lyapunov gains selected were $K = 4$ and $P = 2$. The simulations were executed over 20 orbits.

Table 1 compares the fuel measurement for the Lyapunov and LQR controllers from [6] with the Lyapunov controller from this article. For each deputy compared, both Lyapunov controllers consumed the same amount of fuel to maintain the projected-circular formation. This was expected because both controllers perform a similar feedback linearization. This validates the Lyapunov controller from this article. However, the LQR controller from [6] performed much better, mainly because it does not expend the same control effort to cancel out nonlinear dynamic terms. With perfect internal models, the two Lyapunov controllers admit zero

TABLE 1. Comparison of Maintenance Fuel Consumption for Lyapunov Controller with the Literature

	Fuel measure as defined in equation (40) (m^2/s^3/year)		
	Lyap (Literature)	Lyap (QRB)	LQR (Literature)
Sat 1	0.0191	0.0191	0.00337
Sat 2	0.0191	0.0191	0.003216
Sat 3	–	0.0191	–
Sat 4	–	0.0191	–

steady state errors. Vaddi and Vadali [6] did not explicitly report the steady state errors obtained with their LQR controller, but rather said they were small because the steady state control effort was small.

Performance with Gravitational Perturbations

In all these simulations, the internal model of the Lyapunov controller was perfect, meaning the feedback linearization term, Υ, perfectly canceled out by the nonlinear dynamic terms. Hence, formation-keeping was perfect and the choice of controller gains was irrelevant, as shown in Fig. 2(d). This is not true when the internal model only approximates the gravitational field. Simulations were performed to examine controller performance when the internal model of the gravitational force is imperfect. To do this, the equations of motion were given one set of parameters whereas the controller was given another.

The Lyapunov controller was found not to be susceptible to small errors in the semimajor axis or eccentricity of the chief orbit. However, performance in terms of Δv and steady-state error was affected when the controller did not model the J_2 perturbation. The chief was initially placed on a circular ($e = 0$) orbit. The longitude of ascending node, Ω, argument of perigee, ω, and initial mean anomaly, M_0, were all set to zero, but the inclination was set to $i = 45^\circ$ in order to cause a mean precession of the satellite orbits. For a low-earth orbit with semimajor axis of 7000 km, the circular formation was simulated in the presence of the first three zonal harmonics, J_2 through J_4. As shown in Tables 2, 3 and 4, maintenance Δv, deviation error $\boldsymbol{\rho}$, and orientation error $\boldsymbol{\varepsilon}$ were larger when the controller did not account for J_2. However, the deviation error could still be kept on the order of meters, with the necessary control effort. It is interesting to note that for the same damping ratio, higher gains increased the control authority and kept the errors smaller, whereas for the same proportional gain, a higher damping ratio decreased the Δv consumption because the oscillations in the error were smaller. As an example, Fig. 3 compares the deviation and orientation error over time when the Lyapunov controller does and does not model the J_2 perturbation.

Corrected Spin Rate

The circular formation is only "natural" when gravitational perturbations are absent. So, the Lyapunov controller was simulated again in the presence of the J_2 perturbation, but instead of specifying the natural circular formation with spin rate n, the corrected rate from equation (26) was used, as was done in [17]. The same orbit parameters were used, but simulations were performed for two semimajor

TABLE 2. Maintenance Δv Per Deputy for the Lyapunov Controller with a Perturbed Gravity Model

	Maintenance Δv (mm/s/orbit)			
	a = 7000 km			
	J_2 Modeled	J_2 Not Modeled	J_2 Modeled	J_2 Not Modeled
	$K = 4, P = 2$		$K = 16, P = 4$	
Sat 1	28.6284	31.5055	28.2754	33.4624
Sat 2	32.6976	52.4326	32.0031	43.4897
Sat 3	28.7206	45.8305	31.1289	41.2163
	$K = 4, P = 1$		$K = 16, P = 2$	
Sat 1	31.1313	38.2922	29.5128	42.5548
Sat 2	34.4860	55.7318	32.5199	56.3840
Sat 3	30.6355	53.2628	33.1939	52.5775

axis lengths: with $a = 7000$ km, $\bar{n}_c = 1.0013$ rad/s, and with $a = 14000$ km, $\bar{n}_c = 1.0003$ rad/s. Four deputy satellites were symmetrically distributed within the QRB frame. The Lyapunov controller implemented a perfect internal model of the gravitational force. The nondimensional control gains were selected as $K = 4$ and $P = 2$.

For $a = 7000$ km, Fig. 4 illustrates the relative orbit trajectory followed by the deputies as viewed in the LVLH frame, as well as the control thrusts applied to each deputy, with and without the spin correction. After around 10 orbits, the control thrusts stabilized. Table 5 compares the Δv consumption of the Lyapunov controller with and without the spin correction. For both semimajor axis lengths, there was a reduction in Δv when tracking the modified circular formation

TABLE 3. Maximum Deviation Error Per Deputy for Lyapunov Controller with a Perturbed Gravity Model

	Maximum Satellite Deviation (km)			
	a = 7000 km			
	J_2 Modeled	J_2 Not Modeled	J_2 Modeled	J_2 Not Modeled
	$K = 4, P = 2$		$K = 16, P = 4$	
Sat 1	1.419×10^{-6}	9.388×10^{-4}	7.604×10^{-7}	3.143×10^{-4}
Sat 2	2.839×10^{-6}	1.115×10^{-3}	1.234×10^{-6}	4.253×10^{-4}
Sat 3	2.701×10^{-6}	1.081×10^{-3}	1.238×10^{-6}	4.505×10^{-4}
	$K = 4, P = 1$		$K = 16, P = 2$	
Sat 1	2.378×10^{-6}	1.313×10^{-3}	1.109×10^{-6}	4.750×10^{-4}
Sat 2	4.723×10^{-6}	1.517×10^{-3}	1.944×10^{-6}	6.468×10^{-4}
Sat 3	4.292×10^{-6}	1.432×10^{-3}	1.913×10^{-6}	7.150×10^{-4}

TABLE 4. Maximum Error in Orientation of QRB for Lyapunov Controller with a Perturbed Gravity Model

Maximum Quaternion Error $\|\varepsilon\|$			
a = 7000 km			
J_2 Modeled	J_2 Not Modeled	J_2 Modeled	J_2 Not Modeled
$K = 4, P = 2$		$K = 16, P = 4$	
8.029×10^{-4}	1.307×10^{-3}	5.482×10^{-4}	6.457×10^{-4}
$K = 4, P = 1$		$K = 16, P = 2$	
8.985×10^{-4}	1.435×10^{-3}	4.268×10^{-4}	5.347×10^{-4}

trajectory. Less control effort was needed to maintain this more "natural" formation. It is concluded that this spin correction provides a meaningful performance improvement, without compromising the shape of the satellite formation. It is noted that for the lower orbit, $a = 7000$ km, the effect of J_2 was more pronounced, hence the higher Δv consumption in Table 5.

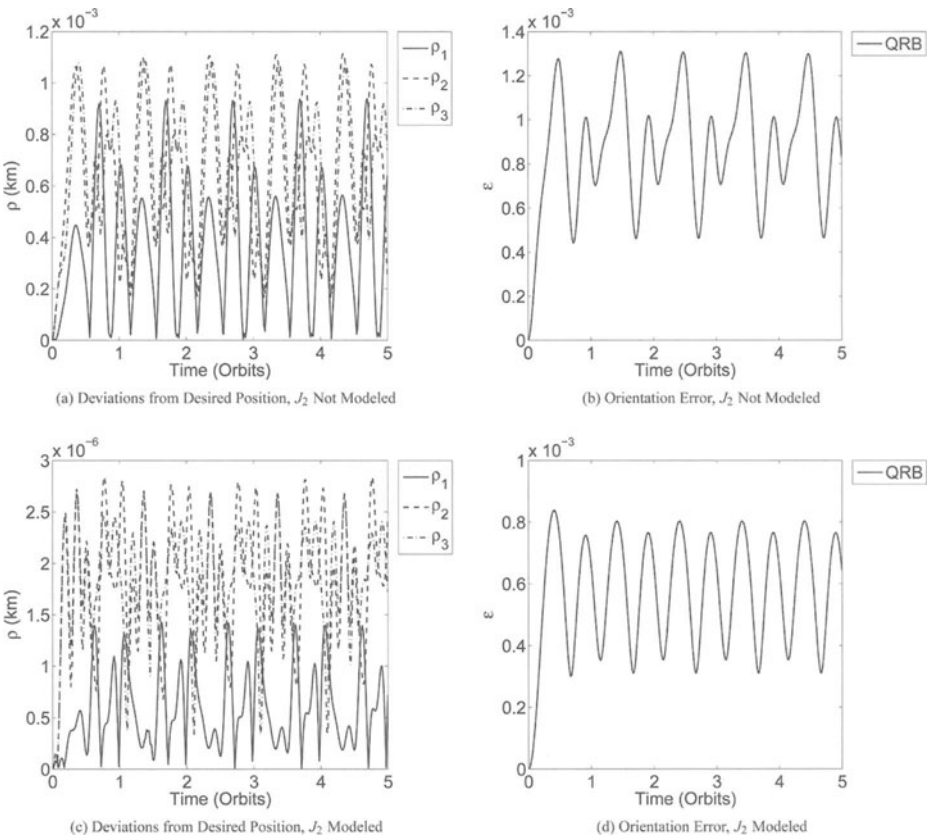

FIG. 3. Comparison of Position and Orientation Error for Different Gravity Models in the Lyapunov Controller $a = 7000$ km, $K = 4$, $P = 2$.

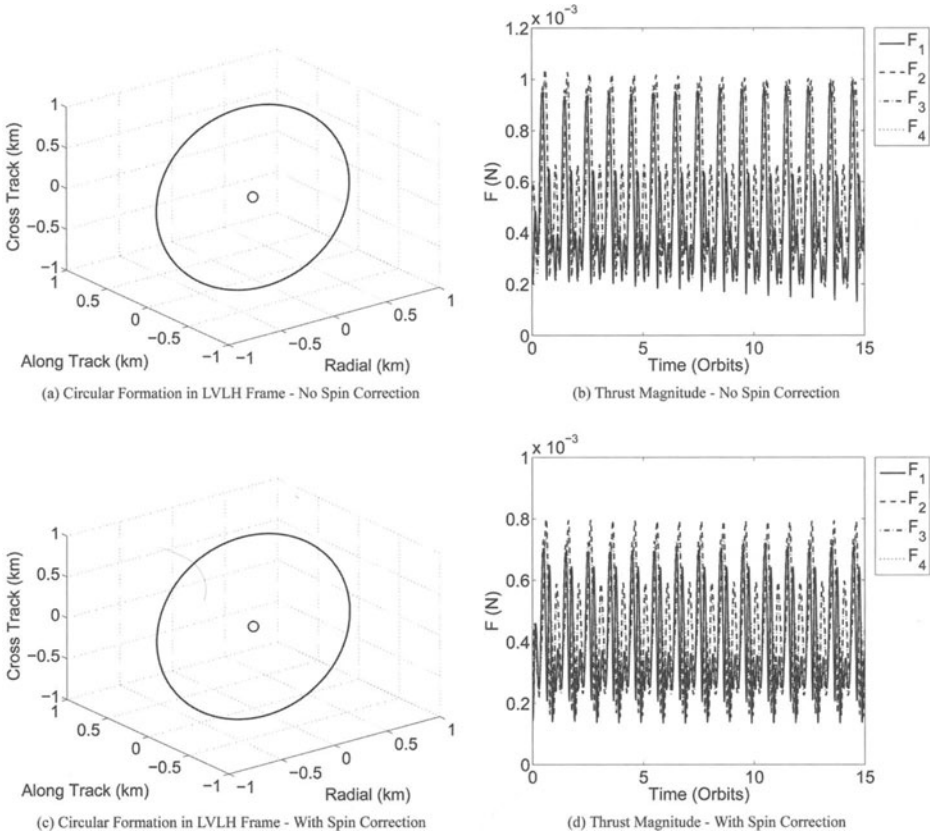

(a) Circular Formation in LVLH Frame - No Spin Correction

(b) Thrust Magnitude - No Spin Correction

(c) Circular Formation in LVLH Frame - With Spin Correction

(d) Thrust Magnitude - With Spin Correction

FIG. 4. Relative Orbits and Control Thrust for "Natural" and "Spin-corrected" Circular Formations, $a = 7000$ km.

To illustrate why this works, Fig. 5 plots the rotation rate of the LVLH frame about its z_H-axis, as obtained from

$$n_{LVLH} = \frac{\|\mathbf{r}_c \times \dot{\mathbf{r}}_c\|}{r_c^2} \tag{41}$$

TABLE 5. Improvement of Maintenance Δv Consumption for Spin-Corrected Circular Trajectory

	Maintenance Δv (mm/s/orbit)			
	a = 7000 km		a = 14000 km	
	n	$\overline{n_c}$	n	$\overline{n_c}$
Sat 1	27.8785	22.8706	2.4893	2.0176
Sat 2	32.9285	26.6677	2.9345	2.3921
Sat 3	27.8832	23.0417	2.4774	2.0405
Sat 4	32.1925	25.6642	2.8010	2.2115

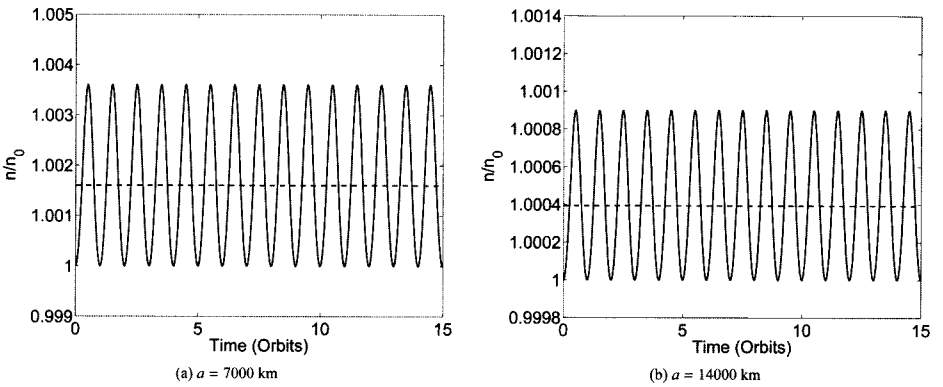

(a) a = 7000 km (b) a = 14000 km

FIG. 5. LVLH Frame Spin Rate in the Presence of J_2 as Calculated from the Chief's Inertial State.

For both semimajor axes, the rate, n_{LVLH}, was larger than the initial mean orbital rate, $n_0 = \sqrt{\mu/a^3}$. For $a = 14000$ km, the average rotation rate over one orbit was 1.0004 rad/s, which matches the spin-correction. For $a = 7000$ km, the average rate of 1.0017 rad/s did not agree as well. Because a natural circular formation also rotates at the orbital rate, the spin-correction compensates for the average increase in orbital rate caused by J_2. However, the correction still ignores the periodic variation around the average that is observed in Fig. 5, so in fighting this, the controllers end up consuming fuel. Vadali et al. [17] introduced filters on the LQR controller that they designed in order to remedy this effect, but such measures are left to future work.

Summary and Conclusion

This article has extended the work of Cochran et al. [13] in developing a novel description of a satellite formation called the QRB formulation. Equations of motion for a formation were derived and it was shown that natural circular formations are conveniently expressed using the formulation. Formation control can effectively be separated into rigidity control and attitude control and a nonlinear Lyapunov controller was designed to accomplish this. Simulations showed that it compares well with a similar controller from the literature. Through proper gain selection, the controller is effective in the face of gravitational perturbations, particularly when the rotational rate to be tracked by the circular formation is modified to account for the J_2 perturbation. The QRB formulation is a useful tool for formation-level controller design.

The QRB formulation is a general tool, and so was not developed with a specific mission in mind. However, to be effective in real-life mission situations, the simplifying assumptions in the Lyapunov controller design would have to be removed and their effect analyzed. In real missions, thrust is not applied in a continuous manner, maximum thrust is limited, and navigation errors affect controller stability. Communication requirements between satellites, data processing, and the on-board implementation of the control scheme would also have to be considered. These are all areas for future work.

Viewing a satellite formation as quasi-rigid means the formulation can be used to design reorientation maneuvers and controllers to execute them [14]. and a subsequent article by the authors explores such maneuvers and the fuel efficiency gained by using the QRB formulation.

Acknowledgment

The authors would like to acknowledge the financial support of the National Science and Engineering Research Council of Canada.

References

[1] HILL, G.W. "Researches in the Lunar Theory," *American Journal of Mathematics*, Vol. 1, No. 1, 1878, pp. 5–26.

[2] WILTSHIRE, R.S. and CLOHESSY, W.H. "Terminal Guidance for Rendezvous in Space," *Journal of Aerospace Science*, Vol. 27, No. 9, 1960, pp. 653–658.

[3] SABOL, C., BURNS, R., and MCLAUGHLIN, C.A. "Satellite Formation Flying Design and Evolution," *Journal of Spacecraft and Rockets*, Vol. 38, No. 2, 2001, pp. 270–278.

[4] YEH, H.-H. and SPARKS, A. "Geometry and Control of Satellite Formations," *Proceedings of the American Control Conference*, Vol. 1, Chicago, IL, USA, Institute of Electrical and Electronics Engineers, 2000, pp. 384–388.

[5] SCHWEIGHART, S.A. and SEDWICK, R.J. "High-Fidelity Linearized J(2) Model for Satellite Formation Flight," *Journal of Guidance, Control, and Dynamics*, Vol. 25, No. 6, 2002, pp. 1073–1080.

[6] VADDI, S.S. and VADALI, S.R. "Linear and Nonlinear Control Laws for Formation Flying," *Proceedings of the AAS/AIAA Space Flight Mechanics Meeting*, Vol. 114, Advances in the Astronautical Sciences, Ponce, Puerto Rico, Feb. 2003, pp. 171–187.

[7] LAWDEN, D.F. *Optimal Trajectories for Space Navigation*. Butterworths, London, England, 1963.

[8] TSCHAUNER, J. and HEMPEL, P. "Rendezvous zu einem in elliptischer Bahn umlaufenden Ziel," *Astronautica Acta*, Vol. 11, 1965, pp. 104–109.

[9] SCHAUB, H., VADALI, S.R., JUNKINS, J.L., and ALFRIEND, K.T. "Spacecraft Formation Flying Control using Mean Orbit Elements," *The Journal of the Astronautical Sciences*, Vol. 48, No. 1, 2001, pp. 69–87.

[10] REN, W. and BEARD, R.W. "Decentralized Scheme for Spacecraft Formation Flying via the Virtual Structure Approach," *Journal of Guidance, Control, and Dynamics*, Vol. 27, No. 1, 2004, pp. 73–82.

[11] TILLERSON, M., BREGER, L., and HOW, J.P. "Distributed Coordination and Control of Formation Flying Spacecraft," *Proceedings of the American Control Conference*, Vol. 2, Institute of Electrical and Electronics Engineers, 2003, pp. 1740–1745.

[12] CLEMENTE, D.C. and ATKINS, E.M. "Optimization of a Tetrahedral Satellite Formation," *Journal of Space-craft and Rockets*, Vol. 42, No. 4, 2005, pp. 699–710.

[13] COCHRAN, J.E. Jr., AOKI, H., and CHOE, N. "Modeling Closely-Coupled Satellite Systems as Quasi-Rigid Bodies," *Proceedings of the AAS/AIAA Space Flight Mechanics Meeting*, Vol. 119, Advances in the Astronautical Sciences, Maui, HI, USA, Feb. 2004, pp. 1349–1368.

[14] BLAKE, C. "Dynamics and Control of Satellite Formations using a Quasi-Rigid Body Formulation," Master's Thesis, McGill University, Montreal, Quebec, Canada, 2008. http://digitool.library.mcgill.ca:8881/R/-?func=dbin-jump-full&object id=21976&current base=GEN01.

[15] SCHAUB, H. and JUNKINS, J.L. *Analytical Mechanics of Space Systems*. AIAA Education series, American Institute of Aeronautics and Astronautics, Reston, VA, 2003.

[16] SCHAUB, H. and ALFRIEND, K.T. "J(2) Invariant Reference Orbits for Spacecraft Formations," *Celestial Mechanics and Dynamical Astronomy*, Vol. 79, 2001, pp. 77–95.

[17] VADALI, S.R., VADDI, S.S., and ALFRIEND, K.T. "An Intelligent Control Concept for Formation Flying Satellites," *International Journal of Robust and Nonlinear Control*, Vol. 12, No. 2–3, 2002, pp. 97–115.

[18] MUKHERJEE, R. and CHEN, D. "Asymptotic Stability Theorem for Autonomous Systems," *Journal of Guidance, Control, and Dynamics*, Vol. 16, No. 5, 1993, pp. 961–963.